Journal of Applied Physics

AIP Publishing

Stochastic dynamics of substrate non-uniform stiffness affecting molecular adhesion in cell-substrate interface subjected to tensile loading

Chenwei Qi,[1] Juanjuan Zhang,[1] Ana-Sunčana Smith,[2,3] and Long Li[1]
[1)]*Key Laboratory of Mechanics on Disaster and Environment in Western China, Ministry of Education, College of Civil Engineering and Mechanics, Lanzhou University, Lanzhou, Gansu, 730000, China*
[2)]*PULS Group, Institute for Theoretical Physics and Interdisciplinary Center for Nanostructured Films, Friedrich Alexander Univesity Erlangen-Nürnberg, Cauerstrasse 3, Erlangen, 91058, Germany*
[3)]*Group for Computational Life Sciences, Division of Physical Chemistry, Ruđer Bošković Institute, Bijenička cesta, 10 000 Zagreb, Croatia*

(*Electronic mail: longl@lzu.edu.cn (L. Li))

(Dated: 6 April 2023)

The mechanically heterogeneous extracellular matrix (ECM) or tissues widely exist in biological system and are capable of significantly regulating the directional cell migration. However, prior to whole cell movement, how the cell senses these cues from mechanical heterogeneities of ECM or substrate remains unclear at the molecular bond level. To address this issue, we theoretically investigate interface adhesion between a non-uniform stiffness substrate and a rigid plate via a series of receptor-ligand bonds subjected to a tensile loading, by integrating substrate surface deformation described by continuum mechanics approach into the stochastic events of bond dissociation and association govern by Markov processes. Interestingly, it is found that, during stretching adhesion interface, due to the large collective contact forces near the stiff edge of adhesion area, the crack firstly develops at this stiff edge and then grows to another relatively soft adhesion edge until the completed detachment achieved, which is distinct from the cracks growing from both two edges to center of adhesion area in the case of uniformly elastic solid-solid or solid-fluid interface. Moreover, the lifetime of bond cluster, interface adhesion strength and effect of inter-bond distance are examined, respectively. The corresponding mechanism of dependence of the lifetime and adhesion strength on the non-uniform stiffness of substrate and inter-bond distance is also analyzed. These findings provide a detailed mechanistic understanding about the adhesion interface responding to the mechanical heterogeneities of substrate at the molecular bond level.

I. INTRODUCTION

The mechanical cues have important roles in regulating cell behaviors in numerous physiological and pathological processes, such as stem cell differentiation in tissue development,[1,2] collective locomotion of cells in wound healing as well as cancer cell migration in tumor metastasis.[3] In these processes, as living matters cells actively sense and respond to mechanical cues from their surrounding mechanical microenvironments via cell adhesion that relies on the intermittent interaction between a variety of receptor-ligand pairs.[4] One notable example of such a mechanical cue is the ECM stiffness differing considerably between and within tissues.[5] Indeed, the ECM widely exhibits heterogeneity in mechanical properties instead of uniform stiffness due to dynamic cellular interactions and remodeling processes, e.g., transient collagen crosslinking and dynamic fiber network structure organization.[6–8] For instance, in tumor tissue, enhanced crosslinking and specific arrangement triggers local ECM stiffening that gives rise to the heterogeneity of stiffness in the tumor microenvironment.[9,10] Another biological circumstance is the neural crest (an embryonic cell population) self-generating a stiffness gradient in the adjacent tissue.[11]

During cell-ECM or cell-tissue interaction, cell deforms its opposing ECM or tissue with mechanical heterogeneity through cell-generated traction force transmitted by a series of receptor-ligand bonds. In turn, as observed in a variety of artificial biomimetic systems with a comparable degree of substrate stiffness gradient, this mechanical stimuli of mechanically heterogeneous ECM/tissue is able to guide the directional cell migration obviously.[2,3,11–16] Specifically, employing a distinct soft-to-stiff interface consisting of two juxtaposed hydrogels, Lo et al[12] originally explored the directional movement of fibroblasts from the soft to the stiff region on the substrate, called durotaxis. Moreover, regarding cancer cell adhesion on a biomimetic substrate (integrating two-layered distinct elastic hydrogels with lenticular surface topology) associated with anisotropic stiffness gradient, it is found that cancer cells migrate along the orientation parallel to the maximum stiffness of substrate.[17] In addition to mechanically heterogeneous hydrogel substrates, the cell durotaxis is also demonstrated when the micropillar substrates of rigidity gradient is adopted.[18,19] Although it has been suggested that the cells are significantly sensitive to the stiffness gradient substrate at the single-cell scale, prior to whole cell movement how adhesion interface of cell and substrate responds to these mechanical heterogeneities remains elusive at the molecular bond level.

Essentially, during cell-substrate interaction, the molecular bond forming and breaking are highly stochastic and reversible processes. Referring to these characteristics of molecular bonds, extensive efforts have been conducted to address dynamics of molecular bond clusters[20–23] and their response to external mechanical stimulus, such as dynamic loading,[24–27] substrate elasticity or viscosity,[28–31] substrate surface morphology,[32] membrane fluctuations,[33,34] hydrodynamic impact from the blood flow[35–38] and membrane surface tension.[39] Nevertheless, these attentions are mainly focused

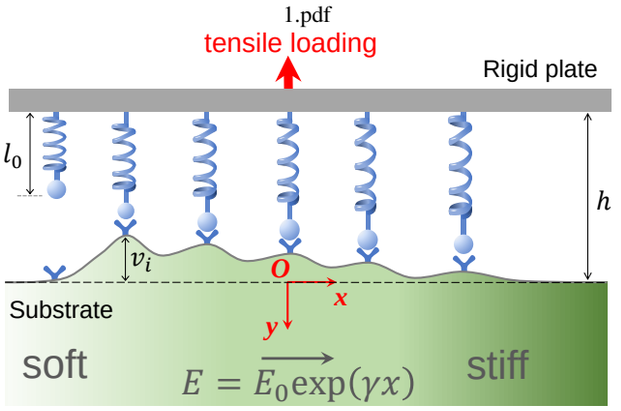

FIG. 1. Schematic diagram of a rigid plate adhering to a non-uniform stiffness substrate mediated by molecular bond cluster under tensile loading. The black dash line indicates the substrate surface at unstressed state. Here the substrate elasticity is introduced based on the simplest form of an exponential function approximately corresponding to the experimental cases.[12,13,17]

on a mechanically homogeneous interface with uniform stiffness or a rigid interface. Given a uniformly elastic substrate, it has been both experimentally and theoretically elaborated that a stiffer substrate provides a more stable interface adhesion of molecular bond clusters subjected to uniform loading since all adhesive bonds share the external loading force more equally in the case of stiffer substrate.[28,40,41] Despite these efforts, the important characteristics of interface adhesion (e.g. adhesion strength, crack propagation as well as lifetime of adhesive bond cluster) is still unknown under dynamic loading when the locally stiff and soft regions appear simultaneously in the context of mechanically heterogeneous substrate.

Difficulty here in theoretically describing the mechanically heterogeneous interface adhesion via receper-ligand bonds depends on integrating the surface deformation of heterogeneous substrate into the stochastic binding and unbinding kinetics of receptor-ligand pairs. As inspired by previously continuous deformable-discrete stochastic framework,[42] in this paper, combining the continuum mechanics and statistical thermodynamics, we investigate the interface adhesion among non-uniform stiffness mediums mediated by molecular bond cluster under tensile loading.

II. THEORETICAL METHOD

In order to understand how the cell interacts with their mechanically heterogeneous ECM at the scale of adhesive molecular bonds, a simple mechanical plane-strain model accounting for the effect of substrate elasticity gradient is presented. Concretely, a rigid plate adheres to a laterally non-uniform stiffness substrate through a series of receptor-ligand bonds subjected to tensile loading as schematically depicted in Fig. 1. Here, corresponding to the experimental cases[12,13,17] in which the substrate elasticity approximately exponentially increase from 1 kPa to 40 kPa, the Young's modulus of substrate exponentially varies in the lateral direction (x coordinate axis) as

$$E(x) = E_0 \exp(\gamma x) \tag{1}$$

with the constant value E_0 at $x = 0$ and a nonhomogeneity constant γ. Clearly, the positive and negative sides of axis x associate with the relatively stiff and soft regions of substrate, respectively. The uniformly distributed adhesive bonds with interval b are represented by a set of thermally elastic springs with rest length l_0 and stiffness λ. The cluster consists of N receptor-ligand bonds.

A. Substrate surface deformation

Concerning the mechanical contact problem between a single rigid punch and such laterally non-uniform stiffness substrate, the surface stress distribution is computationally explored.[43–45] Referring to this mechanical circumstance, we equivalently treat the interplay between individual receptor-ligand bond and substrate as the single bond exerting an distributed pulling pressure on substrate surface during tensile process. In order to obtain the substrate surface deformation while all intermittent bonds deform the substrate together, in the following, we first briefly describe the single bond pulling the substrate and subsequently yield the surface deformation of substrate in the case of molecular bond cluster based on superposition principle.

For pulling the substrate via a single bond, under the coordinate system as shown in Fig. 1, the equilibrium equations with respect to the displacement components (u, v) of substrate in the x- and y- directions can be expressed as[43,44]

$$\begin{aligned}&(\kappa+1)\frac{\partial^2 u}{\partial^2 x}+(\kappa-1)\frac{\partial^2 u}{\partial^2 y}+2\frac{\partial^2 v}{\partial x\partial y}+\gamma(\kappa+1)\frac{\partial u}{\partial x}\\&+\gamma(3-\kappa)\frac{\partial v}{\partial y}=0,\end{aligned} \tag{2}$$

$$\begin{aligned}&(\kappa+1)\frac{\partial^2 v}{\partial^2 y}+(\kappa-1)\frac{\partial^2 v}{\partial^2 x}+2\frac{\partial^2 u}{\partial x\partial y}+\gamma(\kappa-1)\frac{\partial v}{\partial x}\\&+\gamma(\kappa-1)\frac{\partial u}{\partial y}=0,\end{aligned} \tag{3}$$

where the constant κ is denoted as $\kappa = 3-4\upsilon$ with the Poisson's ratio υ. Applying Fourier integral transformation technique to the above equilibrium equations gives the general solutions for the substrate displacement components as

$$u(x,y) = \frac{1}{2\pi}\int_{-\infty}^{\infty}\sum_{j=1}^{2} M_j(\rho)\, c_j \exp(\mathrm{i}\rho x + s_j y)\, d\rho, \tag{4}$$

$$v(x,y) = \frac{1}{2\pi}\int_{-\infty}^{\infty}\sum_{j=1}^{2} M_j(\rho) \exp(\mathrm{i}\rho x + s_j y)\, d\rho, \tag{5}$$

where i represents the imaginary unit $\sqrt{-1}$ and the parameters

s_j and c_j ($j=1,2$) are expressed as

$$s_1 = -\frac{1}{2}\gamma\sqrt{\frac{3-\kappa}{\kappa+1}} - \frac{1}{2}\sqrt{4\rho^2+4\mathrm{i}\gamma\rho+\gamma^2\frac{3-\kappa}{\kappa+1}}, \quad (6)$$

$$s_2 = \frac{1}{2}\gamma\sqrt{\frac{3-\kappa}{\kappa+1}} - \frac{1}{2}\sqrt{4\rho^2+4\mathrm{i}\gamma\rho+\gamma^2\frac{3-\kappa}{\kappa+1}}, \quad (7)$$

$$c_j = -\frac{(\kappa+1)s_j^2+\gamma(\kappa-1)\mathrm{i}\rho-(\kappa-1)\rho^2}{[2\mathrm{i}\rho+\gamma(\kappa-1)]s_j}. \quad (8)$$

The other terms, $M_j(\rho)$ with $j=1,2$, in the expression of substrate displacement (as shown in Eqs. 4 and 5), are the unknown parameters to be numerically determined by the boundary conditions.

During a single bond pulling substrate, a general stress boundary condition can be given as

$$\sigma_{yy}(x,0) = p(x),\ \sigma_{xy}(x,0) = 0, \quad (9)$$

with distributed traction $p(x)$ along the substrate surface. Furthermore, the constitutive relation for substrate can be expressed as

$$\sigma_{yy}(x,y) = \frac{E(x)}{2(1+\upsilon)(\kappa-1)}\left[(\kappa+1)\frac{\partial v}{\partial y}+(3-\kappa)\frac{\partial u}{\partial x}\right], \quad (10)$$

$$\sigma_{xy}(x,y) = \frac{E(x)}{2(1+\upsilon)}\left(\frac{\partial u}{\partial y}+\frac{\partial v}{\partial x}\right). \quad (11)$$

Inserting Eqs. (1,4,5 and 9) into above constitutive equations yields

$$\begin{bmatrix} s_1(\kappa+1)+\mathrm{i}\rho(3-\kappa)N_1 & s_2(\kappa+1)+\mathrm{i}\rho(3-\kappa)c_2 \\ \mathrm{i}\rho+s_1c_1 & \mathrm{i}\rho+s_2c_2 \end{bmatrix}\cdot\begin{bmatrix} M_1(\rho) \\ M_2(\rho) \end{bmatrix} = \begin{bmatrix} 2(1+\upsilon)(\kappa-1)\int_{-\infty}^{\infty}\frac{p(z)}{E(z)}\exp(-\mathrm{i}\rho z)\,dz \\ 0 \end{bmatrix}. \quad (12)$$

Solving this linear system obtains the expression of unknown parameters $M_j(\rho)$ containing the surface traction $p(x)$. This contact stress $p(x)$ can be achieved by numerically solving a singular integral equation associated with boundary conditions[43,44]. Especially, during a single bond pulling substrate within a contact zone $-a<x<a$ with the receptor-ligand bond radius a, assuming the uniform substrate surface displacement within the contact zone, we can determine the additional boundary and equilibrium conditions as

$$\frac{\partial v(x,0)}{\partial x} = 0 \ \text{ for } -a<x<a, \quad \int_{-a}^{a}\sigma_{yy}(x,0)\,dx = P, \quad (13)$$

where P stands for the pulling force exerted on the substrate via single receptor-ligand bond. Combining the displacement of Fourier expression in Eq. 4 and above additional boundary and equilibrium conditions in Eq. 13 derives the singular integral equation of the second kind with respect to the unknown contact stress $p(x)$ that can be subsequently calculated by numerically solved the conducted singular integral equation based on the expansion-collocation method. This numerical solution procedure has been considerably described in previous literature[43–45] for classical contact problem, please see details in these related works.

Once the contact stress $p(x)$ induced by single receptor-ligand bond pulling is obtained, the surface deformation $v(x,0)$ depending on pulling force P can be calculated by using Eqs. 4 and 12. When a set of receptor-ligand bonds give rise to the substrate deformation, the surface deformation profile of substrate can be acquired through superposition principle due to the linear stress-strain relations and linear strain-displacement relations treated for the elastic substrate in the current context.

B. Finite element method

To verify above numerical predictions on surface deformation. Based on the finite element method (FEM), the software COMSOL Multiphysics is adopted to analyze the deformation of the non-uniform stiffness substrate under a tensile loading. The transversal gradient substrate is treated with Young's modulus (E) increasing with the length direction, see Eq. 1 for details. There is a tensile loading in the center of the top of the transversal gradient material. Since the bond pulling substrate is treated as interaction between a non-uniform stiffness half-space and a flat contact in the present theoretical model, to have a fair comparison, the tensile loading first acts on an elastic block of homogeneous material with a much larger stiffness around 80 GPa, close to a rigid flat tip, and further deforms the substrate. This elastic block is perfectly bonded with the transverse gradient substrate to guarantee that the stress is fully transferred to the transverse gradient substrate. In the calculation, the solid mechanics module is used to analyze its deformation. The left, right, and bottom sides of the transverse gradient substrate are fixed constraints, and its upper side is free. For the elastic block, only longitudinal displacements are allowed on the left and right sides. Then the triangular elements are used for meshing, and it contains 635 domain elements (the convergence is verified). Finally, the steady-state solver is used to solve this problem. During the computational process, it is also worth noting that the computational calculations of substrate deformation significantly depend on the size of elastic body. Specifically, for a large elastic body, there has no evident boundary deformation so that the computational results on substrate deformation are approximately close to the theoretical predictions. However, when the size of elastic body is small, the possible boundary deformation calculated based on FEM would give rise to a large difference in computationally calculated and theoretically predicted substrate deformation. In order to effectively simulate deformation of a half-space elastic substrate, an appropriate size of elastic body is hence chosen to avoid boundary deformation taking place in the FEM simulations.

C. Stochastic dynamics of adhesive interface

Given the effective bond density, $1/b^2$, a slice of the system with out-of-plane b is considered in a simple way. As the bond formed by receptor binding to its ligand and the unbinding of receptor-ligand pairs indeed are stochastic processes,

TABLE I. Representative system parameters used in the current context.

Quantity	Meaning	Value
υ	Poisson's ratio of substrate	0.3
γ	Elastic nonhomogeneity constant	10^{-3} 1/nm
E_0	Constant Young's modulus	10 kPa
l_0	Rest length of bond	11 nm[46]
λ	Bond stiffness	0.25 pN/nm[47]
a	Bond radius	1 nm[48]
b_0	Distance constant	32 nm[28]
b	Interval between binding sites	$0.5b_0$, b_0 and $2b_0$
ε_b	Binding affinity	$5\,k_BT$[49]
α	Reaction radius	1 nm[4]
k_0	Intrinsic reaction rate	2×10^4 s^{-1}[50]
N	Total number of bonds	31, 60

the adhesion configuration of molecular bond cluster would be evolved over time by random bond association and dissociation events. For any possible transient adhesion configuration in the context of interface adhesion of the non-uniform stiffness substrate and the rigid plate system mediated by molecular bond cluster under tensile loading, the substrate surface deformation corresponding to transient equilibrium of adhesion system can be determined by the geometric and force equilibrium conditions as

$$v_i+\Delta_i+l_0=h\quad(i=1\cdots n)\quad\text{and}\quad\sum_{i=1}^{n}f_i=F,\tag{14}$$

where u_i indicates the substrate surface deformation at the i-th bond position x_i and on the basis of superposition principle can be defined as $v_i=\sum_{j=1}^{n}v_{ij}$ with the displacement v_{ij} at x_i induced by the force f_j transmitted through the j-th bond located at x_j. At this moment the relationship between the force $f_j=P_jb$ and the substrate surface displacement v_{ij} is numerically determined as described in the above subsections. The terms $\Delta_i=f_i/\lambda$, h and F reflects the stretched length of the i-th bond, the separation between two surface at undeformed position and the total loading force, respectively. For this possible adhesion configuration, n means the total number of the closed receptor-ligand bonds. The unknown $n+1$ parameters $(f_i,\cdots f_n,h)$ or $(f_i,\cdots f_n,F)$ would be calculated by solving Eq. 14 for force-controlled or displacement-controlled loading. Correspondingly, the related substrate surface profile would be obtained. For such substrate surface profile, each receptor-ligand pair state would stochastically transfer between the bound and unbound states, govern by the association and dissociation rates as[22,50,51]

$$k_{\text{on}}=k_0\sqrt{\frac{\lambda\alpha^2}{2\pi k_BT}}\exp\left[-\frac{\lambda}{2k_BT}\left(\delta-l_0-\alpha\right)^2\right],\tag{15}$$

$$k_{\text{off}}=k_0\exp\left(-\frac{\varepsilon_b}{k_BT}\right)\exp\left(\frac{2\lambda\alpha\Delta-\lambda\alpha^2}{2k_BT}\right),\tag{16}$$

with the intrinsic reaction rate k_0, the distance δ between two surfaces, the reaction radius α of binding site, the bond affinity ε_b, the Boltzmann constant k_B and the absolute temperature T.

For a rigid interface, based on Markov process the stochastic process of receptor-ligand bond binding/unbinding can be theoretically described by the relevant master equation whose analytical solution can be readily obtained.[22,46] However, when receptor-ligand bond cluster bridges the elastic mediums, the master equations are significantly complex owing to the large number of all possible adhesion configurations raised by the elastic deformation of substrate. Alternatively, we propose the Monte Carlo simulation to computationally solve the stochastic process on the basis of the first reaction method derived from the Gillespie algorithm[52]. The main steps of simulation procedure are briefly summarized as following. Initially, we assume that all receptor-ligand pairs are bounded. For each individual binding site, the related reaction rate normalized by k_0 can be calculated from Eqs. 15 or 16 as $k_i=k_{\text{off}}/k_0$ for a bound bond or $k_i=k_{\text{on}}/k_0$ for a unbound bond, respectively. Then, randomly generating a set of independent random number w_i with uniform distribution in the interval of [0,1] for all binding sites, we define the time incremental dt corresponding to the next reaction taking place as $dt=\frac{1}{k_0}\min\left\{-\frac{\ln w_i}{k_i}\right\}\quad(i=1,2,\cdots,N)$. Record the reaction site inducing the time incremental and change its bond state from bound to unbound or from unbound to bound. The bond cluster evolution can be obtained by repeating the above procedure. The related system parameters are listed in Table I, in which the substrate Young's modulus within ad-

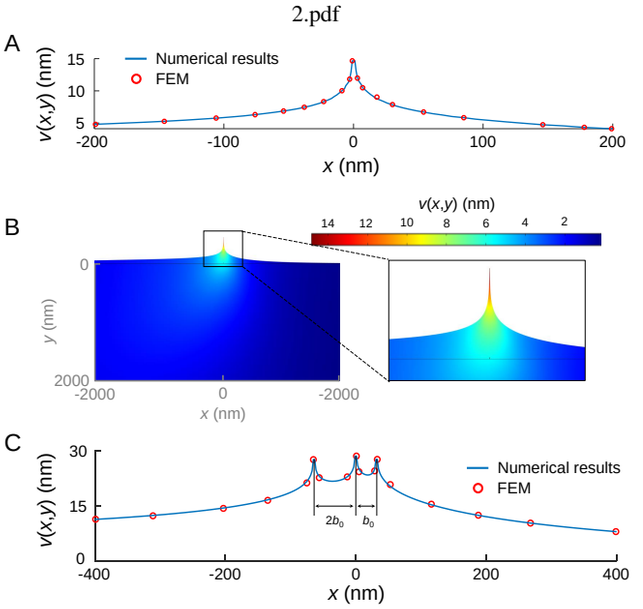

FIG. 2. (A) Substrate surface deformation distribution resulted from tensile loading $P=1$ pN per thickness b_0 transmitted by single bond at $x=0$. (B) The related displacement field $v(x,y)$ computed by finite element method. Here, the presented elastic body is a part of the whole body. (C) Substrate surface deformation induced by tensile forces through three bonds with different inter-bond distance, b_0 and $2b_0$. Three tensile forces act on the substrate surface positions of $x=-2b_0$, 0 and b_0, respectively, and have identical value of $P=1$ pN per thickness b_0.

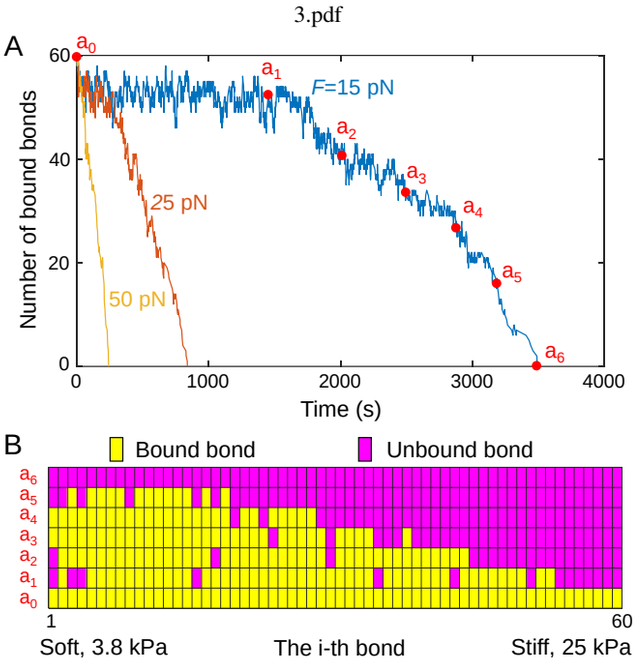

FIG. 3. (A) Evolution of number of bound bonds with time for $N = 60$, $b = b_0$ and different tensile force of 15, 25 and 50 pN. $a_0 - a_6$ stands for the representative cluster configuration states chosen from simulated trajectory of tensile force, 15 pN. (B) Bond state map related to the simulated trajectory points of tensile force, 15 pN. The horizontal coordinate corresponds to the order of receptor-ligand bonds positioned along the adhesion interface as shown in Fig. 1.

hesion zone approximately changes from 3.8 kPa to 25 kPa close to the range of substrate stiffness in the experimental conditions.[2,15,16]

III. RESULTS AND DISCUSSIONS

In order to evaluate the numerically predicted surface deformation of the laterally non-uniform stiffness substrate, we perform the corresponding finite element simulation as mentioned in above section. Fig. 2 shows a comparison of the numerical prediction in the current context and the computational result from finite element simulation on the substrate surface deformation in the cases of a single (Fig. 2A and B) and multiple (Fig. 2C) receptor-ligand bonds applying tension load to the substrate surface. This comparison exhibits excellent agreement. Additionally, as shown in Fig. 2A and B, the substrate surface deformation clearly presents an asymmetrical distribution under tensile loading via single bond owing to the laterally non-uniform stiffness of substrate. In principle, starting from loading position ($x = 0$ in Fig. 2A and B) the surface deformation displays more rapid decrease along the positive x-axis (toward the stiff substrate surface) than this along the negative x-axis (toward the soft substrate surface). In the following, according to this calculated relationship between surface deformation and tensile loading, we examine the stochastic dynamics of molecular bond cluster in response to the heterogeneous elasticity of substrate.

Considering a set of tensile forces, we define the dynamic trajectory of the number of bound bonds as shown in Fig. 3. It is seen in Fig. 3A that the bond dissociation process dominates the bond cluster dynamics under large tensile force where the bond rebinding rarely takes place. Nevertheless this bond rebinding would be significantly enhanced for a small tensile loading even though the interface adhesion of bond cluster will also eventually disappear. This can be explained by the tensile force exerted on each individual bond is capable of decreasing the effective binding affinity of bond.[51] In addition to the evolution of bound bond number, the bond state map evolving with a series of time points is schematically exhibited in Fig. 3B, in which $a_0 - a_6$ are representative cluster configuration states chosen from the simulation trajectory of loading force $F = 15$ pN as marked in Fig. 3A. It is suggested that the interfacial fracture between the rigid plate and the non-uniform stiffness substrate depends on the heterogeneous elasticity of substrate. Explicitly, as a result of adhesive bond dissociation, the crack initializes only at the adhesive edge corresponding to a relatively stiff interface and then gradually propagates towards the soft interface until the two surfaces are completely detached from each other, whereas, for mechanically homogeneous adhesion interface mediated by receptor-ligand bond under tensile loading, previous efforts indicate that the adhesion failure is triggered by cracks concurrently growing from the both two edges of the adhesion interface towards the center.[27,28,42] This is because, for the non-uniform substrate, the discrete interfacial traction forces supported by receptor-ligand bond cluster seriously become large at only the stiff edge of adhesive interface instead of both two edges at which the traction forces have maximum values in the case of homogeneous substrate. These large traction forces guide the receptor-ligand bond dissociation process.

For a given loading force, the associated lifetime of a relatively unstable bond cluster can be directly extracted from the Monte Carlo simulation trajectory as shown in Fig. 3A. After averaging over the lifetime sample space from 1000 simulations (the convergence verified) for each tensile case, the mean lifetime of bond cluster as a function of tensile force is plotted in Fig. 4 where three typical substrates (non-uniform, uniformly stiff and uniformly soft substrates) are taken into account. With increasing tensile force, the mean lifetime decrease monotonously in all three cases. Regarding to a given tensile force, the mean lifetime under the situation of uniformly stiff substrate always has the maximum value among three cases. Interestingly, for a small tensile loading, the lifetime associated with the non-uniform stiffness substrate (Young's modulus ranging from 3.8 to 25 kPa) is notably larger than that in the case of uniformly soft substrate with Young's modulus 3.8 kPa. In contrast, this circumstance related to uniformly soft substrate shows a larger lifetime of bond cluster when a large tensile force is considered (see Fig. 5 for the representative simulated trajectories).

In order to understand these distinct phenomena sensitive to tensile force, correspondingly we further explore the initially discrete contact force distribution acting on substrate surface

4.pdf

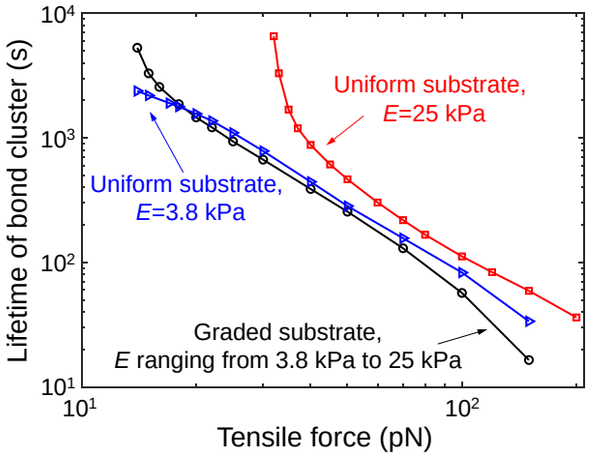

FIG. 4. Lifetime of bond cluster as a function of tensile force in three conditions including uniformly stiff, uniformly soft and non-uniform stiffness substrates for total bond number $N = 60$ and inter-bond distance $b = b_0$.

5.pdf

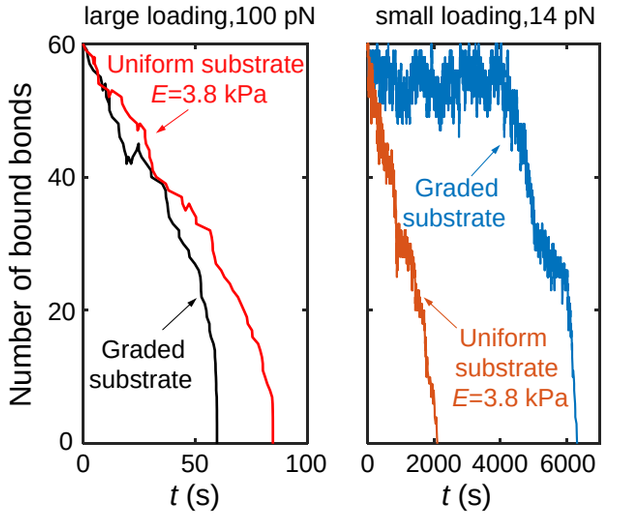

FIG. 5. For uniform and non-uniform elastic substrates, number of bound bonds evolving with time under large and small loading force, respectively, for total bond number $N = 60$ and inter-bond distance $b = b_0$.

via bond cluster as plotted in Fig. 6. During stretching the adhesion interface with a large loading force of 100 pN, although the contact force symmetrically increases from center to both two edges of adhesion area in the case of uniformly soft substrate, the larger collective contact forces from 3.266 to 11.49 pN (labelled through rectangular box in Fig. 6) near the stiff adhesion edge under the situation of the non-uniform stiffness substrate in comparison to uniformly soft substrate give rise to a faster process of adhesion failure. Nevertheless, when the adhesion interface between the non-uniform substrate and the plate is subjected to a small tensile force of

6.pdf

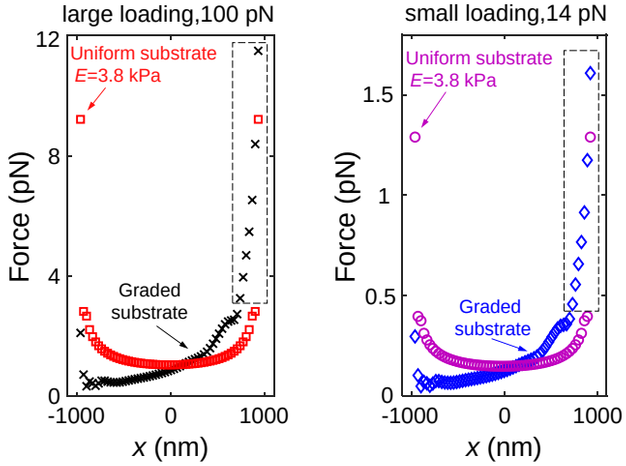

FIG. 6. Referring to the cases as shown in Fig. 5, the initial distribution of discrete contact force under large and small loading force, respectively, in which all receptor-ligand pairs are bound. The rectangular boxes note the collective contact forces near the stiff edge of adhesion interface in the case of the non-uniform substrate.

14 pN, these contact forces gathering near the stiff adhesion edge exactly range from 0.45 to 1.6 pN that is much lower than the characteristic force, 4 pN, required for effectively eliminating the potential well between binder pairs,[53] therefore effectively enhancing the bond association process as shown in Fig. 6. Moreover, for adhesion interface associated with uniformly soft substrate under this small tensile force of 14 pN, the presented collective contact forces at both two edges drive the two cracks simultaneously growing whereas there is only one crack dynamically growing in the case of the non-uniform stiffness substrate. For small tensile force, a lower lifetime of bond cluster related to uniformly soft substrate in comparison to the non-uniform stiffness substrate is a result of these two factors.

In addition to force-controlled loading, we also investigate the stochastic dynamics of adhesion interface between non-uniform stiffness substrate and plate under displacement-controlled loading. Fig. 7A plots the interface tensile force as a function of the change of inter-surface separation $h - l_0$ for different loading rates. The interface tensile force firstly increases and then drops to zero as the change of inter-surface separation increases. The maximum value of this tensile force is identified as the adhesion strength. The higher loading rate, the larger adhesion strength. Furthermore, the dependence of adhesion strength on loading rate is extendedly explored in the three condition including uniformly stiff, uniformly soft and non-uniform stiffness substrates, respectively, as shown in Fig. 7B. All adhesion strengths in these three cases monotonously increase as loading rate increases. When the loading rate tends to zero, the dissociation and association processes of molecular bonds roughly reach equilibrium for any inter-surface separation. Moreover, distinct from the substrate mechanics affecting the relationship between cluster lifetime and tensile loading, as expected for a given loading

7.pdf

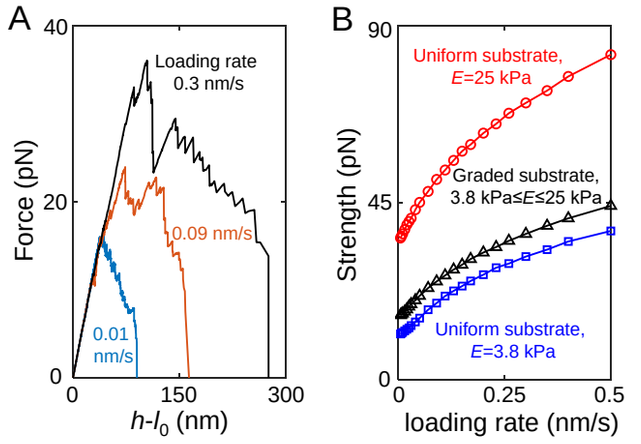

FIG. 7. (A) Dependence of tensile force of non-uniform stiffness substrate interface on the change of inter-surface separation $h - l_0$ under displacement-controlled loading with different loading rate. (B) Referring to three substrate situations (uniformly soft, uniformly stiff and non-uniform substrates), the related adhesion strength as a function of loading rate. Here the system parameters are taken as total bond number $N = 60$ and inter-bond distance $b = b_0$.

8.pdf

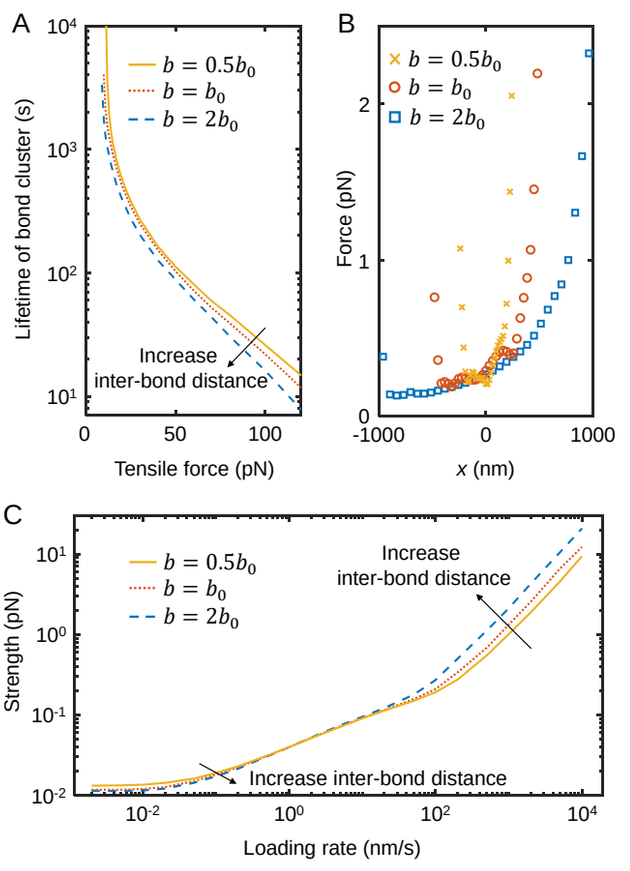

FIG. 8. Effect of inter-bond distance on non-uniform stiffness substrate interacting with rigid plate via molecular bonds. (A) Average lifetime of bond cluster as a function of tensile force for different inter-bond distances, $0.5b_0$, b_0 and $2b_0$. (B) Referring to these three cases of inter-bond distance, under tensile force of 15 pN, the initial traction force distribution on the substrate surface where all receptor-ligand pairs are bound. (C) Dependence of adhesion strength on loading rate for different inter-bond distances, $0.5b_0$, b_0 and $2b_0$ under displacement-controlled loading.

rate the adhesion strength in the case of non-uniform substrate always has the intermediate value among these three substrate conditions (see Fig. 7B). A large adhesion strength, also the maximum value of tensile force, is related to a relatively high inter-surface separation during the whole stretching process as shown in Fig. 7A. Under this circumstance of a relatively high inter-surface separation, soft substrate can't effectively support the interface adhesion due to the large collective contact force near the adhesion edge. As the cases shown in Fig. 7B, the non-uniform stiffness substrate is much stiffer than the uniformly soft substrate, therefore giving rise to a larger adhesion strength.

Furthermore, we consider more cases with different inter-bond distance to simulate the interface fracture during non-uniform stiffness substrate interacting with rigid plate via molecular bonds subjected to tensile loading. Concretely, a set of receptor-ligand bonds ($N = 31$) are symmetrically distributed around the position $x = 0$ of Young's modulus $E_0 = 10$ kPa. Fig. 8 displays the effect of inter-bond distance on non-uniform stiffness substrate interacting with rigid plate via molecular bond. As shown in Fig. 8A, under force-controlled loading, it is found that a long lifetime of bond cluster is associated with a small inter-bond distance as a result of a large traction force near the contact edge in the case of large inter-bond distance (see Fig. 8B). Moreover, the adhesion strength as a function of loading rate for different inter-bond distances also is examined as shown in Fig. 8C. When the loading rate is low, the adhesion strength decreases as the inter-bond distance increases. Nevertheless, for a high loading rate, the adhesion strength increases monotonically with increasing inter-bond distance. These inter-bond distance effects depending on loading rate might be explained by the dynamic competition between the number of bound bonds and bond extension. For the low loading rate, a large number of bound bonds related to small inter-bond distance mainly gives rise to a high adhesion strength. If the loading rate is high, in the case of large inter-bond distance the locally stiff adhesion region providing a large elastic extension of bond mainly causes a large adhesion strength.

It is also worth mentioning that the cell interacting with its mechanically heterogeneous substrate is a complex process containing multiple subcellular and molecular biophysical processes, e.g., spatiotemporal interplay between actomyosin contractility and adhesion,[54] actin cytoskeleton remodeling,[55] receptor mobility,[27] as well as stress fiber contraction.[56] These factors indeed affect the interplay between cell and its mechanical ECM for a real biological system. However, the aim of the work presented here was to provide an insight into how the interface adhesion consisting of molecular bond cluster responds to mechanical stimuli of mechanically het-

erogeneous substrate. This insight should be related to the biological process of mechanically heterogeneous substrate guiding directional cell migration. In addition to the substrate heterogeneity, it should be noted that heterogeneous parallel-bond adhesion clusters also support a mechanically heterogeneous environment owing to the diversity of receptor-ligand bonds with distinct biomechanical properties.[23] Moreover, in fact, as evidently observed in vitro experiments, directional cell migration is governed by a mechanically heterogeneous substrate with elasticity typically ranging from several kilopascal to a few tens of kilopascal. The explicit distribution of substrate elasticity actually relies on the experimentally prepared complex substrate. The present study is to investigate the substrates exhibiting nonlinear stiffness gradient in which the substrate elasticity approximately exponentially increases.[12,13,17] Nevertheless, recent linear stiffness gradient hydrogels are prepared and used to explore stem cell migration and mechanotransduction.[2] In such linear circumstances, the linear function of substrate elasticity should be alternatively considered, instead of the exponential function.

In the current context, the instantaneous elastic deformation of substrate is actually treated. This situation implies that the dynamics of deformation and recovery of substrate surface is relatively faster than the bond association/dissociation processes. However, if the dynamics of substrate deformation and recovery is comparable to the reaction between receptor and ligand, the interplay between surface relaxation and receptor-ligand reaction likely becomes important. For example, in presence of a viscoelastic substrate, its deformation relaxation can significantly enhance the molecular adhesion.[30]

IV. CONCLUSIONS

In summary, using a stochastic-elasticity coupling framework we have investigated the effects of substrate's gradient elasticity, a common feature existing in cell's environment involving in the biological process, on the interface adhesion via receptor-ligand bond cluster under tensile loading. In our model, by combining the surface deformation of non-uniform stiffness substrate defined by continuum mechanics approach and the reversible bound and unbound processes of bond described by statistic thermodynamics, the stochastic dynamics of stretching the adhesion interface and it's relevant bond cluster can be obtained through implementing Monte Carlo simulations. Results show that the dynamic process of adhesion interface in response to tensile loading significantly relies on the gradient elasticity of substrate. Especially, in contrast with the uniformly elastic substrate, during the process of adhesion failure, the non-uniform stiffness substrate distinctly provides only one crack growing from stiff to soft edges of adhesion area instead of two cracks growing from both edges to center in the case of uniformly elastic substrate. This is caused by in presence of non-uniform stiffness substrate the large contact force deeply collects near the stiff adhesion edge that leads to crack initialization and extension. Moreover, during stretching adhesion interface with force- and displacement- controlled loading, the associated lifetime of bond cluster and interface adhesion strength depending on the non-uniform stiffness of substrate are systemically explored. These findings not only help us understand the mechanical mechanism of interface adhesion via molecular bond cluster in response to tensile loading and but also seem to provide an additional view on understanding how cell migration is guided by the heterogeneous elastic substrate. Nevertheless, there are still several issues that have not been considered in the present study such as energy dissipation from receptor-ligand reaction under different loading rates, clustering and biophysical diversity of adhesive molecules. Due to the bond dissociation and association notably relying on substrate surface deformation, the substrate non-uniform stiffness would affect the clustering of adhesive molecules and couple with the diversity of adhesive molecules. The current model actually doesn't include these issues. However, it seems that introducing the molecule mobility may be capable of addressing how the effect of substrate non-uniform stiffness on clustering of adhesive molecules and interplay between deformation of non-uniform stiffness substrate and biophysical diversity of adhesive molecules.

Additionally, the energy dissipation related to different loading rates plays an important role in biological adhesion. Specifically, during cell rolling adhesion under hydrodynamic stimulate from shear flow, owing to the different pathways of adhesive traction during detaching and approaching processes of two surfaces, the adhesion hysteresis of contacting surfaces leading to energy dissipation can significantly regulate the kinetics of rolling adhesion of cell.[36,37] However, because a large fluctuation towards the absorbing boundary inevitably leads to a runaway process, it is difficult to directly obtain the approaching process of two contacting surfaces from the current Monte Carlo simulations. Moreover, since we currently focused on tensile fatigue of the adhesive interface, regarding the non-uniform elastic substrate, the adhesion hysteresis induced by the different pathways of adhesive traction during two surfaces advancing and receding is worthy of future investigation.

V. ACKNOWLEDGMENT

This study is supported by grants from the National Natural Science Foundation of China (12072137) and the Open Fund of Key Laboratory for Intelligent Nano Materials and Devices of the Ministry of Education NJ2020003 (INMD-2021M03). J.Z. would like to acknowledge the support by the Fundamental Research Funds for the Central Universities (Grant No. lzujbky-2022-19).

VI. AUTHOR DECLARATIONS

A. Confict of interest

The authors have no conflicts to disclose.

B. Author Contributions

Chenwei Qi: Formal analysis (lead); Investigation (equal); Methodology (supporting); Validation (equal); Visualization (lead); Writing – original draft (lead). **Juanjuan Zhang:** Software (lead); Writing – review editing (supporting); **Ana-Sunčana Smith:** Conceptualization (supporting); Writing – review editing (supporting). **Long Li:** Conceptualization (lead); Formal analysis (supporting); Funding acquisition (lead); Investigation (equal); Methodology (lead); Project administration (lead); Supervision (lead); Validation (equal); Writing – review editing (lead).

VII. DATA AVAILABILITY

The data that support the findings of this study are available from the corresponding author upon reasonable request.

[1]L. G. Vincent, Y. S. Choi, B. Alonso-Latorre, J. C. Del Álamo, and A. J. Engler, "Mesenchymal stem cell durotaxis depends on substrate stiffness gradient strength," Biotechnology journal **8**, 472–484 (2013).
[2]W. J. Hadden, J. L. Young, A. W. Holle, M. L. McFetridge, D. Y. Kim, P. Wijesinghe, H. Taylor-Weiner, J. H. Wen, A. R. Lee, K. Bieback, *et al.*, "Stem cell migration and mechanotransduction on linear stiffness gradient hydrogels," Proceedings of the National Academy of Sciences **114**, 5647–5652 (2017).
[3]B. J. DuChez, A. D. Doyle, E. K. Dimitriadis, and K. M. Yamada, "Durotaxis by human cancer cells," Biophysical journal **116**, 670–683 (2019).
[4]E. A. Evans and D. A. Calderwood, "Forces and bond dynamics in cell adhesion," Science **316**, 1148–1153 (2007).
[5]J. R. Tse and A. J. Engler, "Stiffness gradients mimicking in vivo tissue variation regulate mesenchymal stem cell fate," PloS one **6**, e15978 (2011).
[6]A. Malandrino, M. Mak, R. D. Kamm, and E. Moeendarbary, "Complex mechanics of the heterogeneous extracellular matrix in cancer," Extreme Mechanics Letters **21**, 25–34 (2018).
[7]H. Li, J. M. Mattson, and Y. Zhang, "Integrating structural heterogeneity, fiber orientation, and recruitment in multiscale ecm mechanics," Journal of the mechanical behavior of biomedical materials **92**, 1–10 (2019).
[8]M.-J. Chow, R. Turcotte, C. P. Lin, and Y. Zhang, "Arterial extracellular matrix: a mechanobiological study of the contributions and interactions of elastin and collagen," Biophysical journal **106**, 2684–2692 (2014).
[9]M. Plodinec, M. Loparic, C. A. Monnier, E. C. Obermann, R. Zanetti-Dallenbach, P. Oertle, J. T. Hyotyla, U. Aebi, M. Bentires-Alj, R. Y. Lim, *et al.*, "The nanomechanical signature of breast cancer," Nature nanotechnology **7**, 757–765 (2012).
[10]I. Acerbi, L. Cassereau, I. Dean, Q. Shi, A. Au, C. Park, Y. Chen, J. Liphardt, E. Hwang, and V. Weaver, "Human breast cancer invasion and aggression correlates with ecm stiffening and immune cell infiltration," Integrative Biology **7**, 1120–1134 (2015).
[11]A. Shellard and R. Mayor, "Collective durotaxis along a self-generated stiffness gradient in vivo," Nature **600**, 690–694 (2021).
[12]C.-M. Lo, H.-B. Wang, M. Dembo, and Y.-l. Wang, "Cell movement is guided by the rigidity of the substrate," Biophysical journal **79**, 144–152 (2000).
[13]K. Moriyama and S. Kidoaki, "Cellular durotaxis revisited: initial-position-dependent determination of the threshold stiffness gradient to induce durotaxis," Langmuir **35**, 7478–7486 (2018).
[14]J. Dou, S. Mao, H. Li, and J.-M. Lin, "Combination stiffness gradient with chemical stimulation directs glioma cell migration on a microfluidic chip," Analytical chemistry **92**, 892–898 (2019).
[15]C. Kayal, E. Moeendarbary, R. J. Shipley, and J. B. Phillips, "Mechanical response of neural cells to physiologically relevant stiffness gradients," Advanced Healthcare Materials **9**, 1901036 (2020).
[16]P. Tseng and D. Di Carlo, "Substrates with patterned extracellular matrix and subcellular stiffness gradients reveal local biomechanical responses," Advanced Materials **26**, 1242–1247 (2014).
[17]H. Zhang, F. Lin, J. Huang, and C. Xiong, "Anisotropic stiffness gradient-regulated mechanical guidance drives directional migration of cancer cells," Acta Biomaterialia **106**, 181–192 (2020).
[18]L. Trichet, J. Le Digabel, R. J. Hawkins, S. R. K. Vedula, M. Gupta, C. Ribrault, P. Hersen, R. Voituriez, and B. Ladoux, "Evidence of a large-scale mechanosensing mechanism for cellular adaptation to substrate stiffness," Proceedings of the National Academy of Sciences **109**, 6933–6938 (2012).
[19]B. Wang, J. Shi, J. Wei, X. Tu, and Y. Chen, "Fabrication of elastomer pillar arrays with elasticity gradient for cell migration, elongation and patterning," Biofabrication **11**, 045003 (2019).
[20]E. Evans and K. Ritchie, "Dynamic strength of molecular adhesion bonds," Biophysical journal **72**, 1541–1555 (1997).
[21]R. Merkel, P. Nassoy, A. Leung, K. Ritchie, and E. Evans, "Energy landscapes of receptor–ligand bonds explored with dynamic force spectroscopy," Nature **397**, 50–53 (1999).
[22]T. Erdmann and U. S. Schwarz, "Stability of adhesion clusters under constant force," Physical review letters **92**, 108102 (2004).
[23]A. K. Dasanna, G. Gompper, and D. A. Fedosov, "Stability of heterogeneous parallel-bond adhesion clusters under load," Physical Review Research **2**, 043063 (2020).
[24]D. Li and B. Ji, "Predicted rupture force of a single molecular bond becomes rate independent at ultralow loading rates," Physical review letters **112**, 078302 (2014).
[25]U. Seifert, "Rupture of multiple parallel molecular bonds under dynamic loading," Physical review letters **84**, 2750 (2000).
[26]L. Li, H. Yao, and J. Wang, "Dynamic strength of molecular bond clusters under displacement-and force-controlled loading conditions," Journal of Applied Mechanics **83** (2016).
[27]D. Kaurin, P. K. Bal, and M. Arroyo, "Peeling dynamics of fluid membranes bridged by molecular bonds: moving or breaking," Journal of the Royal Society Interface **19** (2022).
[28]J. Qian, J. Wang, and H. Gao, "Lifetime and strength of adhesive molecular bond clusters between elastic media," Langmuir **24**, 1262–1270 (2008).
[29]J. Wang and H. Gao, "Clustering instability in adhesive contact between elastic solids via diffusive molecular bonds," Journal of the Mechanics and Physics of Solids **56**, 251–266 (2008).
[30]L. Li, W. Zhang, and J. Wang, "A viscoelastic–stochastic model of the effects of cytoskeleton remodelling on cell adhesion," Royal Society Open Science **3**, 160539 (2016).
[31]Z. Gong, S. E. Szczesny, S. R. Caliari, E. E. Charrier, O. Chaudhuri, X. Cao, Y. Lin, R. L. Mauck, P. A. Janmey, J. A. Burdick, *et al.*, "Matching material and cellular timescales maximizes cell spreading on viscoelastic substrates," Proceedings of the National Academy of Sciences **115**, E2686–E2695 (2018).
[32]S. Yu, H. Wang, Y. Ni, L. He, M. Huang, Y. Lin, J. Qian, and H. Jiang, "Tuning interfacial patterns of molecular bonds via surface morphology," Soft Matter **13**, 5970–5976 (2017).
[33]S. F. Fenz, T. Bihr, D. Schmidt, R. Merkel, U. Seifert, K. Sengupta, and A.-S. Smith, "Membrane fluctuations mediate lateral interaction between cadherin bonds," Nature physics **13**, 906–913 (2017).
[34]J. A. Janeš, C. Monzel, D. Schmidt, R. Merkel, U. Seifert, K. Sengupta, and A.-S. Smith, "First-principle coarse-graining framework for scale-free bell-like association and dissociation rates in thermal and active systems," Physical Review X **12**, 031030 (2022).
[35]K.-C. Chang, D. F. Tees, and D. A. Hammer, "The state diagram for cell adhesion under flow: leukocyte rolling and firm adhesion," Proceedings of the National Academy of Sciences **97**, 11262–11267 (2000).
[36]L. Li, H. Tang, J. Wang, J. Lin, and H. Yao, "Rolling adhesion of cell in shear flow: A theoretical model," Journal of the Mechanics and Physics of Solids **119**, 369–381 (2018).
[37]W. Kang, L. Li, and J. Wang, "Synergistic regulation mechanism of selectin and integrin on leukocyte adhesion under shear flow," Journal of Applied Mechanics **89** (2022).
[38]C. Dong and X. X. Lei, "Biomechanics of cell rolling: shear flow, cell-surface adhesion, and cell deformability," Journal of biomechanics **33**, 35–43 (2000).
[39]D. Kaurin and M. Arroyo, "Surface tension controls the hydraulic fracture of adhesive interfaces bridged by molecular bonds," Physical review letters **123**, 228102 (2019).

[40]U. S. Schwarz and M. L. Gardel, "United we stand–integrating the actin cytoskeleton and cell–matrix adhesions in cellular mechanotransduction," Journal of cell science **125**, 3051–3060 (2012).
[41]U. S. Schwarz and S. A. Safran, "Physics of adherent cells," Reviews of Modern Physics **85**, 1327 (2013).
[42]H. Gao, J. Qian, and B. Chen, "Probing mechanical principles of focal contacts in cell–matrix adhesion with a coupled stochastic–elastic modelling framework," Journal of the royal society Interface **8**, 1217–1232 (2011).
[43]S. Dag, M. A. Guler, B. Yildirim, and A. C. Ozatag, "Sliding frictional contact between a rigid punch and a laterally graded elastic medium," International Journal of Solids and Structures **46**, 4038–4053 (2009).
[44]C. Peijian, C. Shaohua, and P. Juan, "Sliding contact between a cylindrical punch and a graded half-plane with an arbitrary gradient direction," Journal of Applied Mechanics **82**, 041008 (2015).
[45]S. Dag, M. A. Guler, B. Yildirim, and A. C. Ozatag, "Frictional hertzian contact between a laterally graded elastic medium and a rigid circular stamp," Acta Mechanica **224**, 1773–1789 (2013).
[46]T. Erdmann and U. S. Schwarz, "Bistability of cell-matrix adhesions resulting from nonlinear receptor-ligand dynamics," Biophysical journal **91**, L60–L62 (2006).
[47]E. Evans, K. Kinoshita, S. Simon, and A. Leung, "Long-lived, high-strength states of icam-1 bonds to $\beta 2$ integrin, i: lifetimes of bonds to recombinant $\alpha 1 \beta 2$ under force," Biophysical journal **98**, 1458–1466 (2010).
[48]P. Carl, C. H. Kwok, G. Manderson, D. W. Speicher, and D. E. Discher, "Forced unfolding modulated by disulfide bonds in the ig domains of a cell adhesion molecule," Proceedings of the National Academy of Sciences **98**, 1565–1570 (2001).
[49]J. Wang, L. Li, Y. Zhang, K. Zhao, X. Chen, H. Shen, Y. Chen, J. Song, Y. Ma, C. Yang, *et al.*, "Synergetic collision and space separation in microfluidic chip for efficient affinity-discriminated molecular selection," Proceedings of the National Academy of Sciences **119**, e2211538119 (2022).
[50]T. Bihr, U. Seifert, and A.-S. Smith, "Multiscale approaches to protein-mediated interactions between membranes—relating microscopic and macroscopic dynamics in radially growing adhesions," New Journal of Physics **17**, 083016 (2015).
[51]M. Dembo, D. Torney, K. Saxman, and D. Hammer, "The reaction-limited kinetics of membrane-to-surface adhesion and detachment," Proceedings of the Royal Society of London. Series B. Biological Sciences **234**, 55–83 (1988).
[52]D. T. Gillespie, "A general method for numerically simulating the stochastic time evolution of coupled chemical reactions," Journal of computational physics **22**, 403–434 (1976).
[53]G. I. Bell, "Models for the specific adhesion of cells to cells: a theoretical framework for adhesion mediated by reversible bonds between cell surface molecules." Science **200**, 618–627 (1978).
[54]B. Rubinstein and I. M. Pinto, "Epithelia migration: A spatiotemporal interplay between contraction and adhesion," Cell adhesion & migration **9**, 340–344 (2015).
[55]R.-M. Mège, J. Gavard, and M. Lambert, "Regulation of cell–cell junctions by the cytoskeleton," Current opinion in cell biology **18**, 541–548 (2006).
[56]A. Besser and U. S. Schwarz, "Coupling biochemistry and mechanics in cell adhesion: a model for inhomogeneous stress fiber contraction," New Journal of Physics **9**, 425 (2007).

Journal of Applied Physics

AIP Publishing

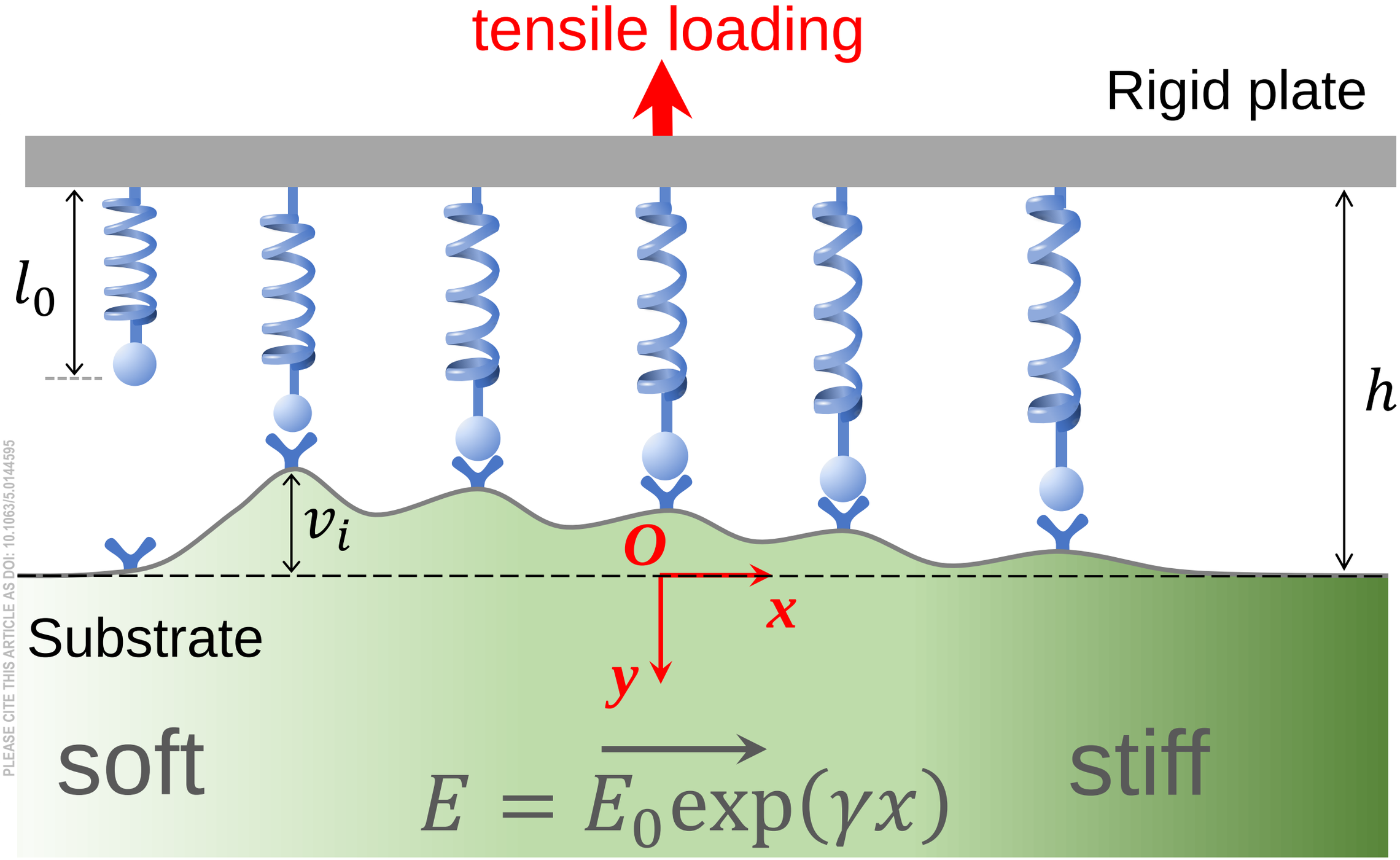

Journal of Applied Physics
AIP Publishing

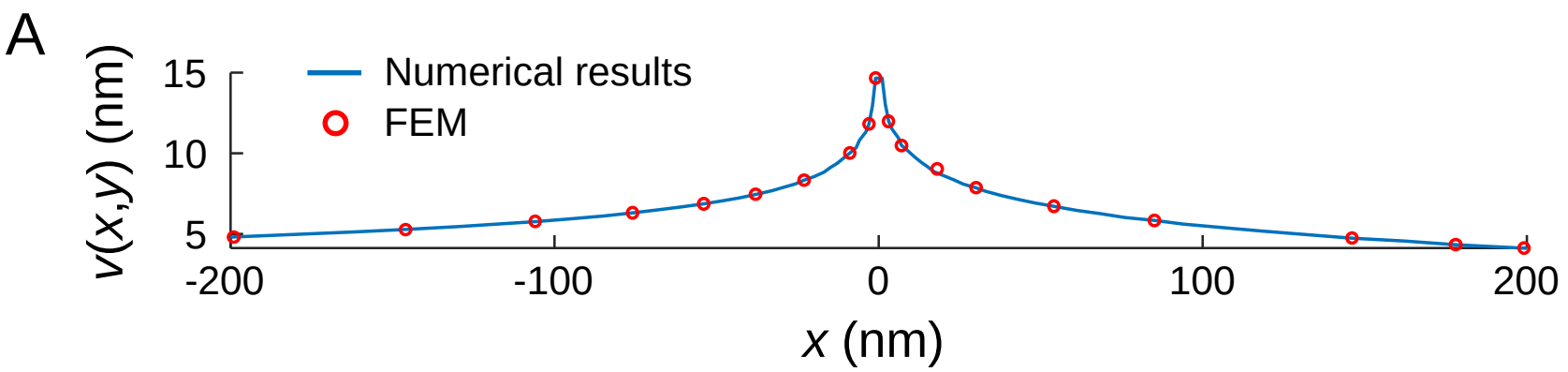

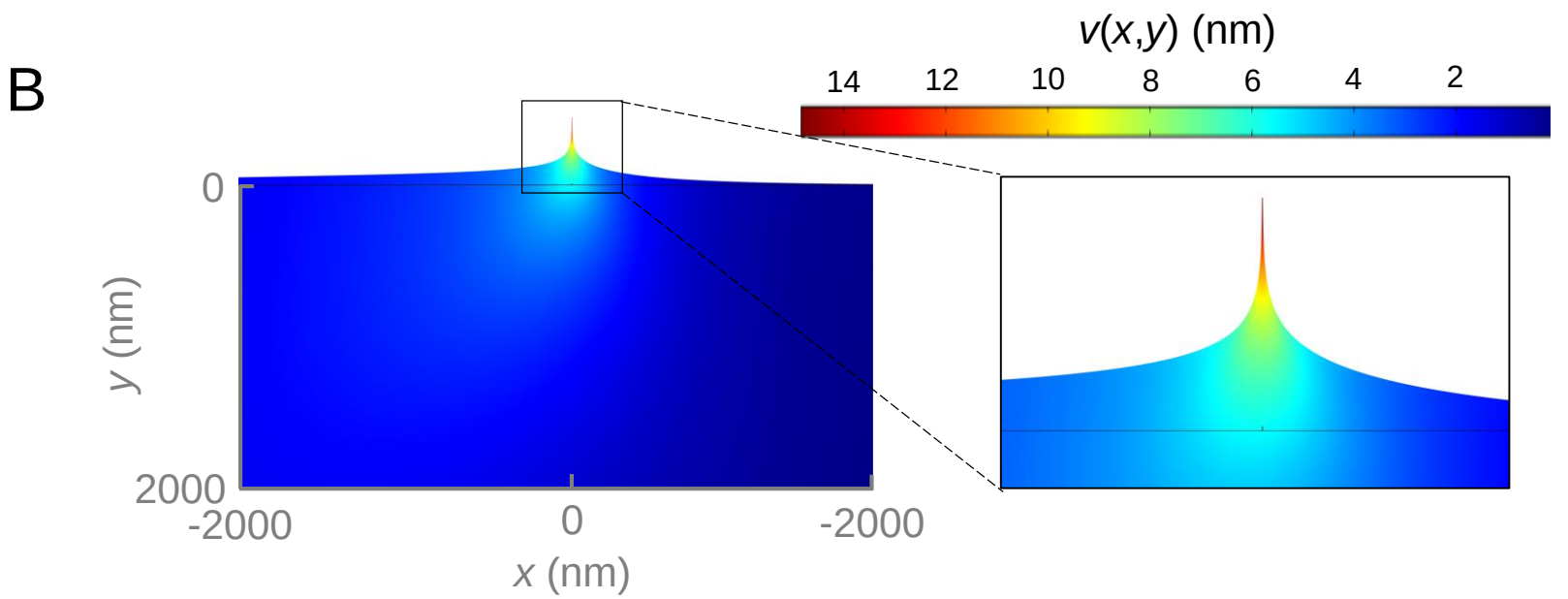

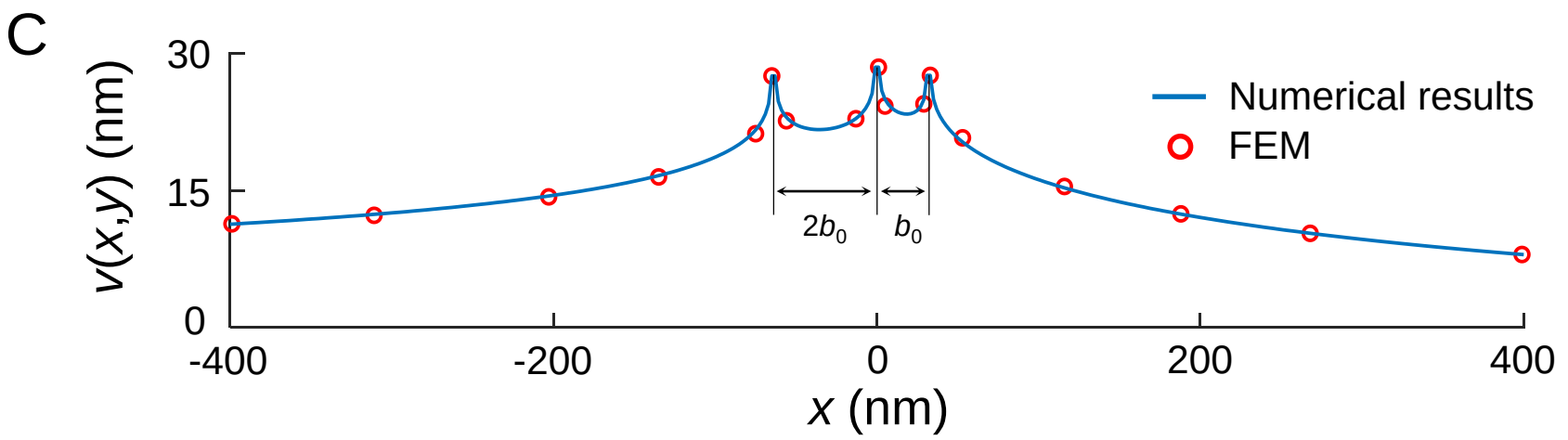

A

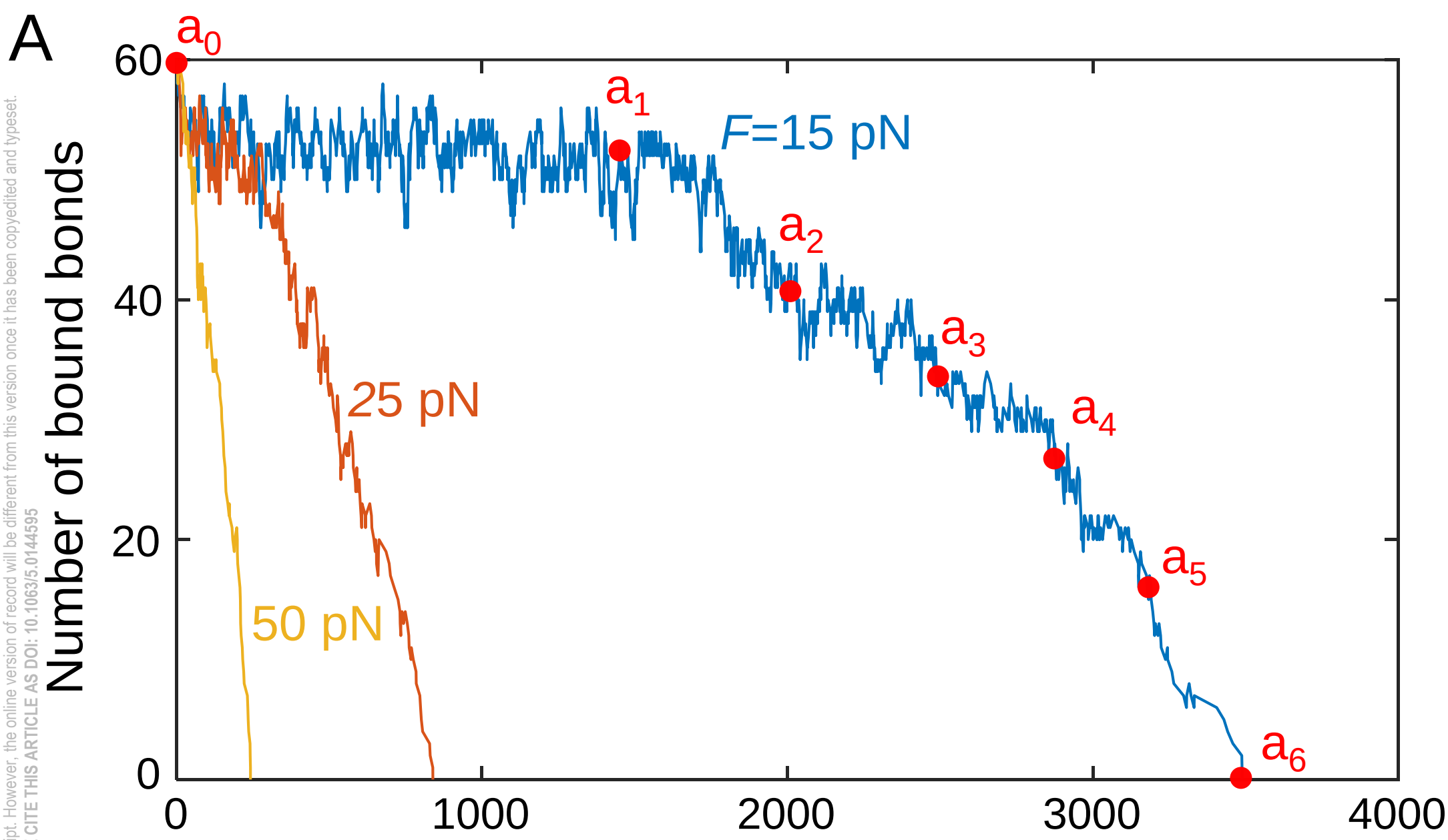

B